Transient solid-phase crystallization study of chemically vapor-deposited amorphous silicon films by *in situ* x-ray diffraction

R. Bisaro
Laboratoire Central de Recherches, Thomson—Compagnie Générale de Télégraphie sans Fil, Domaine de Corbeville, 91404 Orsay CEDEX, France

J. Magariño
Eurodisplay, Domaine de Corbeville, 91404 Orsay CEDEX, France

Y. Pastol
IBM Research Division, Thomas J. Watson Research Center, P.O. Box 218, Yorktown Heights, New York 10598

P. Germain and K. Zellama
Groupe de Physique des Solides de l'Ecole Normale Supérieure, Université de Paris VII, 2 place Jussieu, 75252 Paris CEDEX 05, France

(Received 1 May 1989)

Transient solid-phase crystallization kinetics of undoped silicon films prepared by chemical vapor deposition of silane has been studied with *in situ* x-ray diffraction. The experiments were performed under vacuum in a high-temperature chamber mounted on the θ circle of a step-by-step goniometer. By studying the Bragg-peak-intensity dependence on the isothermal-annealing time (t) over a wide temperature range $594\,^{\circ}\mathrm{C} \leq T \leq 658\,^{\circ}\mathrm{C}$, we have directly determined the volume of the crystallized phase and the grain size. We report direct experimental evidence that solid-phase crystallization occurs first at the substrate-layer interface through the growth of three-dimensional islands after a fast transient heterogeneous nucleation mechanism. We observe a relative crystal-lattice expansion of about 3×10^{-3} at the beginning of this regime. The decrease of the corresponding elastic-energy contribution to the free energy of the system with increasing annealing time enhances the driving force of the amorphous-crystalline phase transition. Our experimental data give indirect evidence of the presence of strained submicrocrystallites in the amorphous phase as a precursor state of the crystalline state. According to the models generally used, a phenomenological sequence describing the solid-phase crystallization kinetics is also given.

I. INTRODUCTION

The crystallization kinetics of *a*-Si layers has been the subject of many studies using different techniques on materials prepared by several methods: evaporation, ion implantation, and glow discharge.[1–7] Structural models have been proposed to satisfactorily explain the orientation[8–11] or the doping aspects of the growth.[7,12–14] If the amorphous-crystalline phase transition must be regarded as a first-order transition, as the discontinuity in the observed experimental physical properties proves it,[15–18] no direct *in situ* experiments were, however, done to provide evidence in the amorphous phase for a precursor state prior to a crystalline state. The purpose of this work is to study the initial stages of the solid-phase crystallization mechanism of undoped *a*-Si films prepared by chemical vapor deposition (CVD) on fused-silica substrates and annealed under vacuum in the range $594\,^{\circ}\mathrm{C} \leq T \leq 658\,^{\circ}\mathrm{C}$. Solid-phase crystallization, which was already studied by *in situ* x-ray diffraction experiments,[19] is an important part of the crystallization mechanisms operating during the CVD and low-pressure CVD of silicon.[7,11] It also occurs during the processing of the integrated-circuit (IC) devices (e.g., in ion implantation followed by annealing[20]). The use of x-ray diffraction allows us to report here precise measurements of the volume fraction of the crystallized growing phase at each step of the early stages of the crystallization process and experimental evidence of a transient surface-induced heterogeneous nucleation regime.

II. EXPERIMENTAL SETUP

The amorphous films were prepared in a CVD reactor (Applied Material AMV 800) at atmospheric pressure. Pure silane (1 l/min) was diluted in hydrogen (32 l/min) in a vertical open-flow reactor with a silicon carbide susceptor heated by rf induction. We used fused-silica substrate held at 600 °C in order to obtain totally amorphous films. The substrates were carefully out-gassed and cleaned by *in situ* HCl etching prior to deposition. The thickness of the layers, 1.3 μm, was measured optically by standard transmission experiments.

The crystallized-volume fraction measurements were performed on as-deposited samples in a high-temperature chamber[19] mounted on the θ circle of a standard θ-2θ Seifert MZ-IV step-by-step goniometer in vertical position. The variations of the x-ray diffraction intensity were measured *in situ* as a function of the annealing time. Measurements were made in the classical Bragg-Brentano

geometry (θ-2θ) in steps of 0.005°. Cu $K\alpha$ radiation and a scintillation detector were used. As-deposited samples were heated by radiation and conduction, using tantalum heating elements. The temperature was monitored using two thermocouples attached to opposite corners of the sample, and was controlled to ±1 °C. The chamber is evacuated using a turbo molecular pump. The pressure inside the chamber was less than 10^{-5} Torr. The samples were annealed under vacuum at temperatures in the range $594\,°C \leq T \leq 658\,°C$.

III. EXPERIMENTAL RESULTS

A. Determination of the crystallized-volume fraction from *in situ* x-ray measurements

We assumed that crystallization from the amorphous phase occurs by the construction of an ideally imperfect crystal from tiny fragments. These fragments were assumed to be so small that each extracts only a negligible amount of energy from the x-ray beam. In this situation no phase relationship will exist between the waves reflected from the fragments and the complete reflection will be the sum of the intensity contributions from the individual fragments. In this situation the well-known kinematical theory of x-ray diffraction applies, and the integrated intensity P_{hkl} from each fragment is proportional to its volume dV. An absolute determination of the crystallized volume requires the collection of data on all the (hkl) planes. Measurements of diffraction were performed always from the (111) planes. It was already shown[11,19] that samples crystallized in this way exhibit a strong ⟨111⟩ preferred orientation of growth. We defined[11] the ⟨111⟩ character by the calculated ratios

$$\alpha_i = C_p / C_i \quad \text{and} \quad \beta_i = C_p' / C_i' \ , \tag{1}$$

where $C_i = A_{(220)} / A_{(111)}$ and $C_i' = A_{(311)} / A_{(111)}$ are ratios of Bragg-peak intensities collected on the samples, C_p and C_p', those collected on a standard randomly oriented sample. α_i and β_i are constant for the whole crystallization process. At the onset of the crystallization no signal could be collected on (220) and (311) planes. The integrated intensity of diffracted peaks on (111) planes gives a value proportional to the crystallized volume. If the integral width β remains constant during annealing, the grain size normal to (111) is constant and the height of the Bragg peak gives a measured value proportional to the number of crystalline fragments formed from the amorphous phase. The kinetics of solid-phase crystallization was determined unambiguously from the dependence of the intensity of the Bragg peak on the isothermal annealing time.

B. Results

In Fig. 1 we present an example of a (111) Bragg-peak dependence on the isothermal annealing time t_A. Annealing times for complete crystallization of the films range from 32×10^3 to 1.4×10^3 s, depending on T_A. In Figs. 1(a) and 1(b) the (111) Bragg peak is emerging from the first amorphous halo of a-Si. The peak grows with time at an annealing temperature T_A of 609 and 613 °C, respectively. The starting peaks are always shifted up to about 0.09° (2θ) towards low angles. In Fig. 1(c) crystallization is almost completed at $T_A = 613\,°C$. The integral linewidth remains systematically constant throughout the temperature and annealing time ranges. The average grain size in the ⟨111⟩ direction is about 60 nm.

In Figs. 2(a) and 2(b) we present examples of the dependence of the normalized diffracted intensity on the annealing time for crystallizations performed at four different temperatures at the onset of the crystallization: 627, 612, 604, and 594 °C [Fig. 2(a)], until the complete crystallization [Fig. 2(b)].

Figure 3 represents the dependence of $y = \log_{10}\{\ln[1/(1-x)]\}$ versus $\log_{10}$ (annealing time t), where x is the crystallized volume fraction. Figure 3 shows that the experimental Bragg intensity and hence the volume of the crystalline phase exhibits a linear variation for almost the whole annealing time. This linear variation was previously interpreted[19] and had provided a measurement of the crystallization regrowth rate

$$V_g(T) = V_g^0(C_d)\exp(-E_v / k_B T) \ , \tag{2}$$

where E_v is the activation energy of the regrowth rate, $E_v \cong 3.1$ eV, and $V_g^0(C_d)$ an increasing function of the doping level C_d.

At the onset of the crystallization there is a departure from the linear dependence. Figure 3 shows that during the lower times ($t < \tau_s^a$), when $x \ll 1$, $y \cong \log_{10} x$ remains constant or varies very slightly. After this regime, y rapidly increases as a γt^3 function.

Figure 4 shows the variation of $\log(1/\tau_s^a)$ as a function of the reciprocal absolute temperature; the slope yields an activation energy of 3.3 eV.

IV. DISCUSSION

Crystallization in amorphous materials occurs through the nucleation and the growth of crystallites formed during the nucleation process.[21] The growth process occurs via the jump of an atom across an amorphous-crystalline (a-c) phase boundary. The growth rate V_g is usually written

$$V_g = \delta \nu' \ , \tag{3}$$

where δ is the jump distance of an atom at the interface and ν' is a frequency; ν' is the product of an atomic frequency for atomic vibrations by a thermal activated[21] term which describes the probability of the atomic jump,

$$\nu' = (k_B T / h)\exp(-\Delta g^* / k_B T) \ . \tag{4}$$

The variation $\Delta G^s(r)$ of the Gibbs free energy due to the transformation of m atoms from the amorphous phase into a crystallite of m atoms is written as the sum of a bulk and a surface term. These terms being of opposite sign, $\Delta G^s(r)$ has a maximum value $\Delta G^{s*}(r)$. The model of steady-state nucleation considers that stable crystallites are created when crystal nuclei have grown to reach a critical size r^*. It is, however, important to note at this stage of the discussion that from a thermodynami-

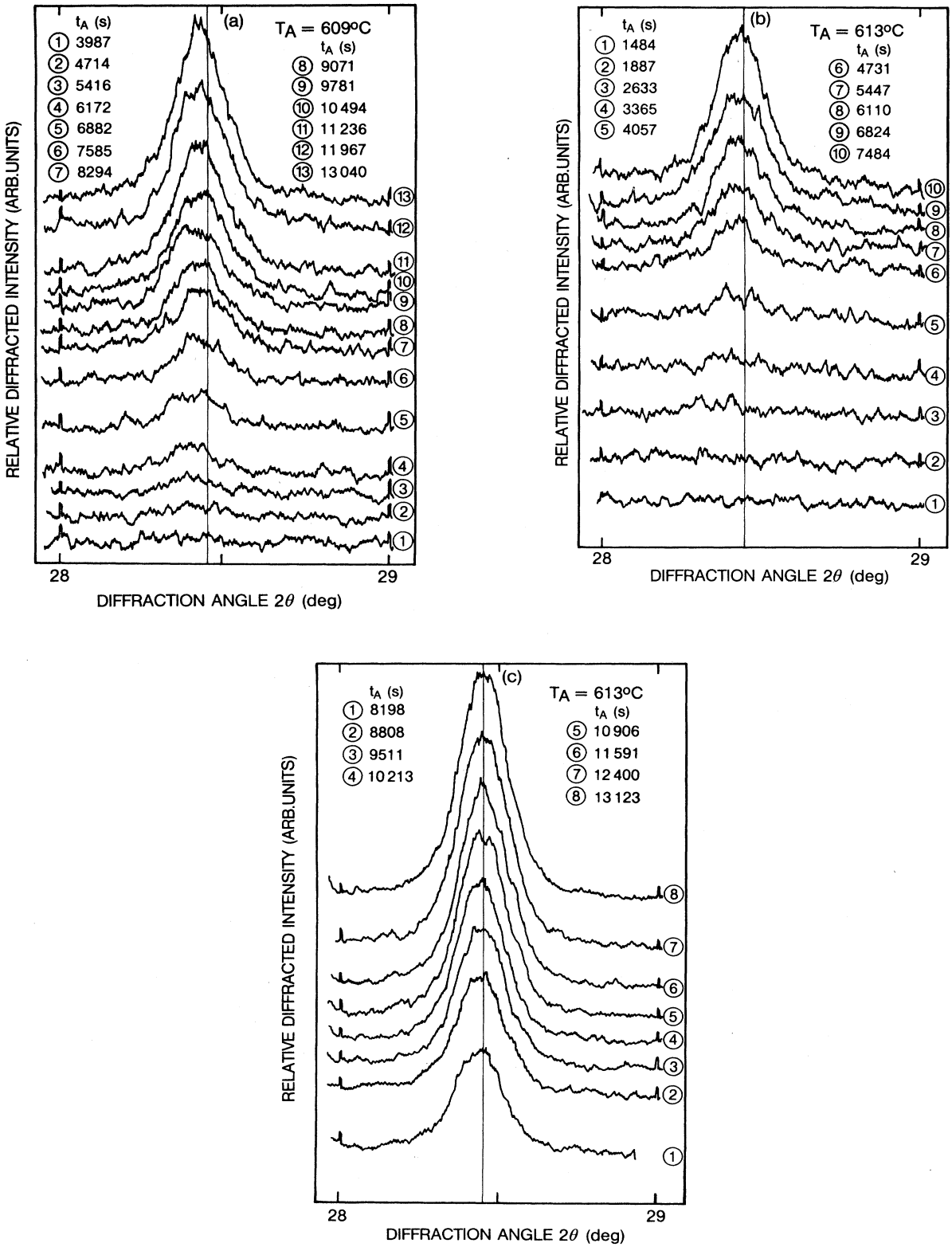

FIG. 1. Dependence of the diffracted intensity on the (111) planes on the annealing time (t_A) at annealing temperature $T_A = 609$ and 613 °C. For each spectrum, the maximum intensity of the Bragg peak is measured at annealing time t_A. Annealing times increase from the bottom to the top of the figure. (a) and (b) The onset of the crystallization at $T_A = 609$ and 613 °C, respectively. The starting peaks are shifted towards low angles. The vertical line indicates the position of the Bragg peak at the end of the crystallization process. (c) The end of the crystallization at $T_A = 613$ °C.

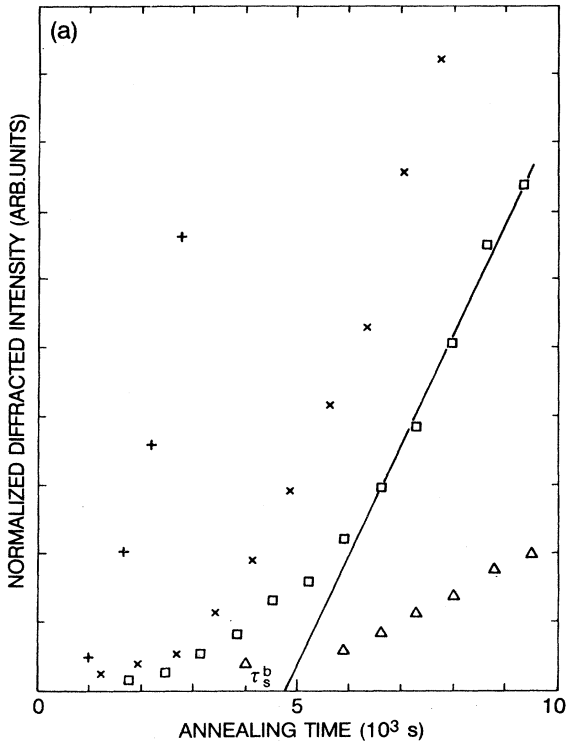

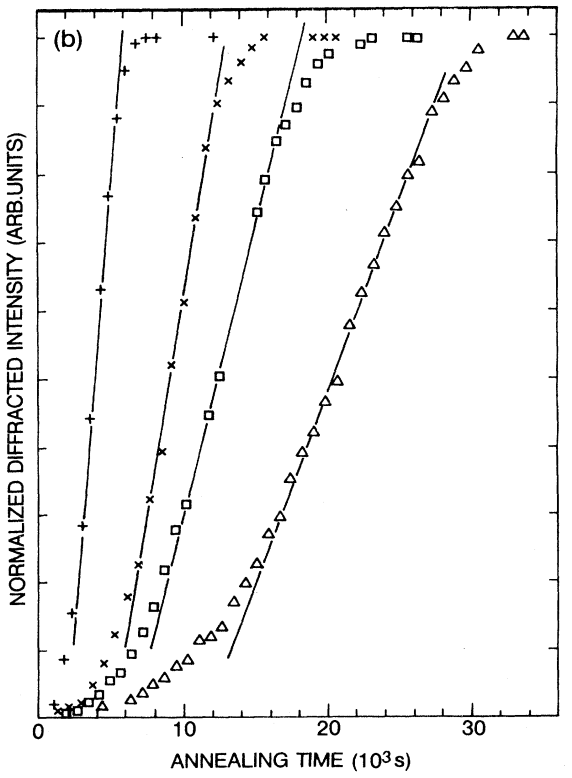

FIG. 2. Dependence of the normalized diffracted intensity on t_A at T_A of +, 627 °C; ×, 612 °C; □, 604 °C; Δ, 594 °C. (a) The onset of the crystallization. (b) Until complete crystallization.

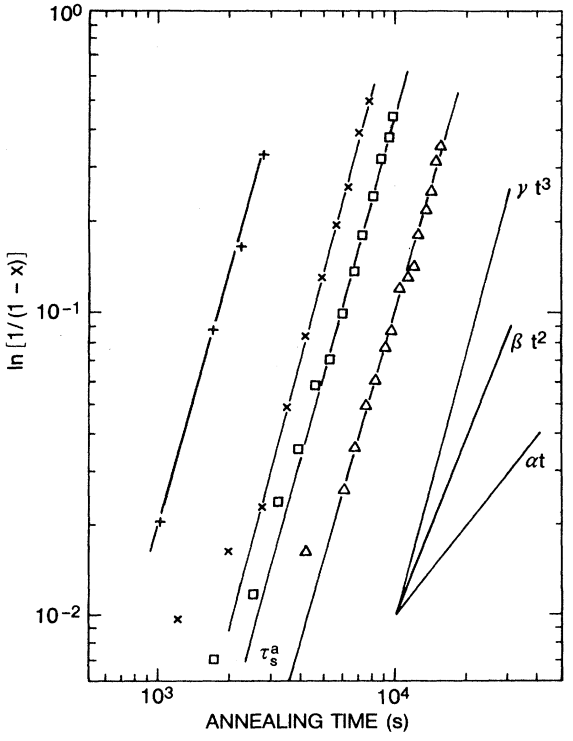

FIG. 3. Dependence of $y = \log_{10}\{\ln[1/(1-x)]\}$ vs $\log_{10}(t_A)$ at T_A of +, 627 °C; ×, 612 °C; □, 604 °C; Δ, 594 °C.

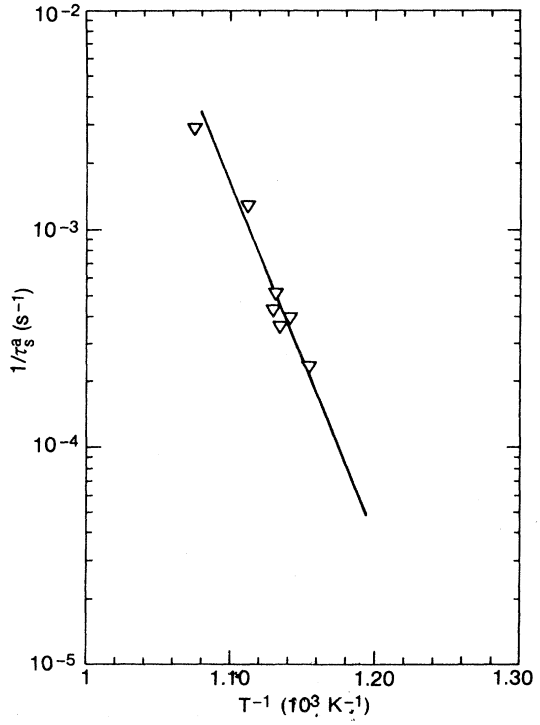

FIG. 4. Variation of $\log_{10}(1/\tau_s^a)$ as a function of the reciprocal absolute temperature; the slope yields an activation energy of 3.3 eV.

cal point of view, clusters of atoms may be stable even though their size r is smaller than r^*, if their structure is not crystalline. We had shown earlier[7,11] that surface-induced nucleation occurs at the substrate–a-Si interface. In the case of heterogeneous steady-state nucleation occurring on a solid substrate s and a shape of spherical cap making a characteristic contact angle θ (Fig. 5), Turnbull[22] showed that

$$\Delta G^s(r)=(\pi r^2\sigma_{ac}+\pi r^3/3\,\Delta G_v)g(\theta)\ , \tag{5}$$

where ΔG_v is the variation of the Gibbs free energy for the transformation $a\rightarrow c$ per unit volume ($\Delta G_v<0$), r is the radius of the crystallite, $g(\theta)=[2(1-\cos\theta)-\sin^2\theta\cos\theta]$, $\cos\theta$ is defined by the expression $\cos\theta=-(\sigma_{cs}-\sigma_{as})/\sigma_{ac}$, where $\sigma_{ac},\sigma_{cs},\sigma_{as}$ are the surface free energies of a-c,c-s,a-s interfaces, respectively.

The maximum of $\Delta G^s(r)$ occurs at $r=r^*$:

$$r^*=-2\sigma_{ac}/\Delta G_v\ . \tag{6}$$

It has been previously assumed (steady-state nucleation) that the steady-state concentration of clusters exists at all times. However, at the very beginning of the transformation, there must be a finite (transient) period of time during which the steady-state concentration is established. A simplified expression which gives the transient period to within roughly an order of magnitude of the nucleation rate, for heterogeneous nucleation $R^s(t)$ is the expression

$$R^s(t)=R^s_\infty\exp(-\tau^a_s/t)\ , \tag{7}$$

where R^s_∞ is the steady-state nucleation rate, i.e., the number of stable crystallites which appears per unit time in an untransformed volume unity containing N atoms,

$$R^s_\infty=N\nu'\exp[-\Delta G^{s*}(r)/k_BT]\ . \tag{8}$$

The time τ^a_s is interpreted in terms of a transient heterogeneous nucleation regime during which the steady-state concentration of crystalline stable nuclei at the annealing temperature is established at the substrate-film interface. According to Germain *et al.*[23]

$$\tau^a_s=i^{*2}_s/(n^*_s\nu')\ , \tag{9}$$

where i^*_s is the number of atoms in the crystallite of critical size and n^*_s is the number of atoms at the surface of the crystallite which are available for a jump across the a-c interface

$$\tau^a_s=(i^{*2}_s\delta/n^*_s)/V_g=\lambda/V_g\ . \tag{10}$$

The quantities i^*_s and n^*_s are not independent but correspond to the same crystallite of critical size. As the parameter i^*_s probably has weak dependence on temperature[23], and δ is almost constant, then λ depends very weakly on T. It follows that V_g and $1/\tau^a_s$ should have roughly the same activation energy. This is what we experimentally observe. Figure 4 shows that $1/\tau^a_s$ is thermally activated with an activation energy of 3.3 eV close to that of V_g (3.1 eV) and similar to activation energies measured by Zellama *et al.*[24] for bulk-induced crystallization.

If $n^*_s=(i^*)^{2/3}$, $i^*\cong(\lambda/\delta)^{3/4}$, and the calculated number of atoms i^*_s in a critical nucleus is found to be about 100 for $\delta=3.13$Å. The corresponding diameter of a critical nucleus is about 20 Å. Figure 4 shows that after this regime, y rapidly increases as a γt^3 function. This corresponds to the formation of isolated three-dimensional polycrystalline islands at the substrate-film interface at the beginning of the crystallization.

The crystallized volume $V_c(t)$ of an isothermal process can be expressed by the relation[25]

$$V_c(t)=V_0\{1-\exp[-V_e(t)/V_0]\}\ , \tag{11}$$

where V_0 is the total volume of the considered sample and $V_e(t)$ the volume defined by Avrami.[26,27] $V_e(t)$ includes all the crystallites which would have been nucleated in the amorphous phase if it had not been already transformed and all the crystallized regions which grow independently and can overlap each other.

If $x(t)=V_c(t)/V_0$, then

$$\ln\{1/[1-x(t)]\}=V_e(t)/V_0\ .$$

$V_e(t)$ comes first from the p_1 crystallites of size a_0 already present at $t=0$. If we assume that they grow in three-dimensional space with a crystallization growth rate V_g and a hemispherical shape, their volume is given by the expression

$$V^a_e(t)=(p_1/2)\tfrac{4}{3}\pi(a_0+V_gt)^3\ . \tag{12}$$

$V_e(t)$ comes secondly from the p_2 crystallites of critical size a_c created during the transient heterogeneous nucleation

$$V^b_e(t)=(p_2/2)\tfrac{4}{3}\pi(a_c+V_gt)^3\ . \tag{13}$$

A transient heterogeneous nucleation is experimentally observed; the crystallized volume fraction $x(t)$ can be approximated by

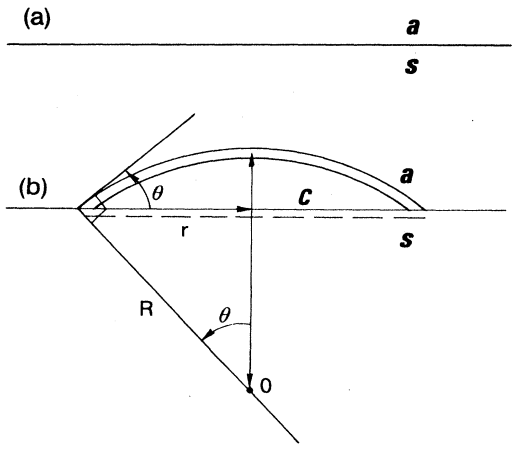

FIG. 5. Schematic cross section of the nucleation of a crystallite at the a-c interface. (a) System before nucleation, (b) system after nucleation: Element of phase c formed from a with a contact angle θ on the surface of the substrate. Line, boundary s-a, free energy σ_{as}; dashed line, boundary s-c, free energy σ_{cs}; double line, boundary a-c, free energy σ_{ac}.

$$x(t)\cong x^b(t)=V^b(t)/V_0=1-\exp[V_e^b(t)/V_0]\ ,$$

hence

$$\ln\{1/[1-x(t)]\}=(p_2/2)\tfrac{4}{3}\pi(a_c+V_g t)^3 V_0^{-1}\ . \qquad (14)$$

The relation (14) agrees very well with our experimental results.

Figures 6(a) and 6(b) show a schematic view of the crystallization process. The three-dimensional heterogeneous growth at the interface is completed for a time $\tau_b^s \ll \tau$ where τ is related to the total thickness of the layer e and to the crystallization rate V_g by the relation $V_g\tau=e$. The regime creates a continuous polycrystalline layer of about 120 nm thick (roughly two superposed grains). When the substrate-layer interface is entirely crystallized, the polycrystalline phase grows perpendicularly to this interface and the crystalline volume is linearly dependent on time.

The shift in the Bragg peak observed during the initiation time is correlated with stresses existing at the amorphous-crystalline interface of the first crystals nucleated. Their contribution diminishes as the volume of the crystalline layer increases with increasing time. At the onset of the crystallization, when an equivalent crystalline continuous layer of 200 Å of thickness is formed at the substrate-amorphous interface, the relative variation of the lattice parameter is about 3×10^{-3}. It vanishes when the linear regime is reached. Veprek *et al.*[18,28] also observed that the lattice parameters of the nuclei of 30 Å of diameter obtained by glow discharge are in tension of about 0.9×10^{-2} to 1.2×10^{-2}. The resulting decrease of the contribution of the corresponding elastic energy to the free energy of the system increases the driving force of the amorphous-crystalline phase transition. Veprek *et al.*[18] stabilized the crystalline phase, which means they obtained smaller particles ($\cong$20 Å), by compressing their films. Important stresses must exist in our films when the critical nuclei of 20 Å of diameter are created. There is a clear experimental correlation between the particle size (the coherence length) and the expansion of the lattice parameter which increases the free surface energy of the crystallites. According to Veprek *et al.*[18] we can calculate the excess internal energy $\delta E(a)$ of an amorphous network, consisting in part (or entirely) of Si-Si pairs in the eclipsed configuration, from the relation

$$\tfrac{9}{2}V_{\text{mole}}B(\Delta d/d_0)^2\cong\delta E(a)-T\,\delta S(a)\ , \qquad (15)$$

where $V_{\text{mole}}=12$ cm^3 is the molar volume of solid silicon, $B=0.99\times10^{12}$ dyne cm^{-2} is the bulk modulus, $\Delta V/V_0\cong3\,\Delta d/d_0$ is the volume expansion, and $\delta S(a)$ is the maximum excess entropy of configuration of continuous random networks used to describe the amorphous phase. Spaepen[29] estimated $\delta S(a)\cong\frac{1}{6}k_B\ln2\cong0.2k_B$ by atom, hence $\delta S(a)\leq0.4$ kcal/mol. In Eq. (15), we neglect the contribution δF(Si-H) of the chemically bonded hydrogen (0.3 at. %) to the free energy of the system. Numerically, we find $\delta E(a)\cong0.55$ kcal/mol. This value is close, first to the intuitively estimated value of 0.6 kcal/mol given by Rudee and Howie[30] using 1.7 kcal/mol of bonds[31] for the barrier of rotation of the molecules H_3C—SiH_3, and secondly to the value of 0.53 kcal/mol calculated by Döhler *et al.*[32] using the adiabatic bond-charge model[33] and six-atom rings.

The important point is not the quite good agreement with the previous determinations but the topological consequences. The amorphous-crystalline phase transition occurs[7,11] with crystallization rates of roughly a few Å/s at temperatures on the order of half the melting point $T_{m/2}$. This fact can be understood because the amorphous phase is built up partly with boat-type six-atom rings. These latter, taken individually or gathered in small clusters, have a free energy F smaller than the corresponding value for seat-type six-atom rings when T reaches 390 K.[32] Progressively, during crystallization, the soft zone-boundary transverse acoustic phonon responsible for the weakness of the c-Si diamond lattice against deformation of the space angle has less anharmonic properties; consequently, the crystalline phase becomes more and more stable.[18] When the cluster size is just smaller than the critical nucleus size, $\leq$20 Å, the cubic diamond-type structure made entirely of seat-type six-atom rings is unstable against others sixfold arrangements, such as boat-type six-atom rings. Mosseri and Sadoc[34] built such a cluster, the unit cell of polytope "240," made of 27 atoms and 18 deformed boat-type six-atom rings. The internal energy of such a cluster is smaller

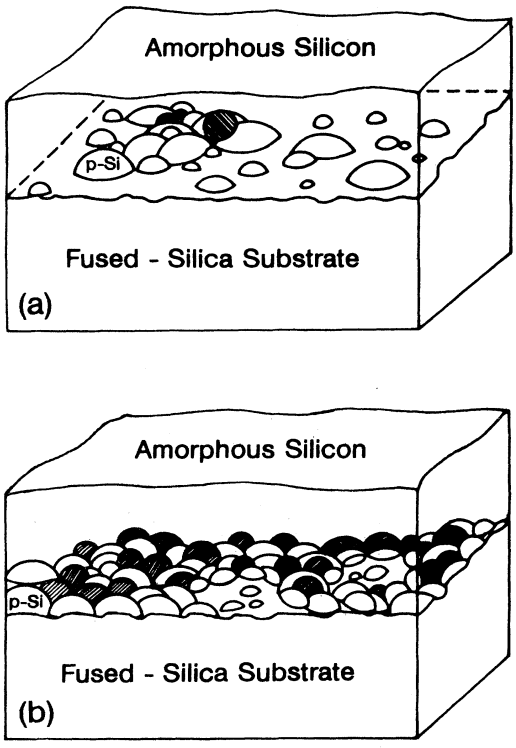

FIG. 6. Schematic view of the crystallization process; (a) the onset of the crystallization, (b) the end of the γt^3 regime.

than that of a cluster of the same size made of Si-Si pairs in the staggered configuration, where only 12 rings are possible. Our work gives indirect experimental evidence that the amorphous-crystalline phase transition occurs through submicrocrystallites.[35,36] We are not able to establish if the submicrocrystalline state is the only description of the amorphous phase or if it is only an intermediate state between the crystalline state and a strained amorphous phase better described by a continuous-random-network model,[37] where the coordination number of atoms is close to 4.0 instead of 2.4 for a strain-free structure.[38,39] A few exacting and comprehensive analyses of informative data support the submicrocrystallite model.[8] It seems important, however, to mention that one way to accommodate the different models for the best understanding of the solid-phase crystallization kinetics of undoped[11] and doped[7] *a*-Si is to consider the submicrocrystalline state not only as a precursor state to the crystalline state but also to suppose that it is created during deposition.

The phenomenological approach of the solid-phase crystallization for boron-doped *a*-Si prepared by CVD can hence be the following. The doping is realized[7,40] by addition of diborane with silane in the gas phase during deposition. The boron-doping concentration, defined by the ratio $C_B=[B_2H_6]/[SiH_4]$, was within $0\leq C_B \leq 2\times 10^{-3}$.

For $0\leq C_B \leq 8.5\times 10^{-6}$, according to Phillips[8], the dangling bonds of the faces of the cluster of the submicrocrystalline model are saturated by hydrogen atoms and the $10^{19}/cm^3$ dangling bonds measured[7] by EPR are on the cluster edges. Boron is incorporated during deposition on the cluster edges, where the reaction (16) occurs:

$$Si_{III}^{0}+B_{III}^{0}\rightarrow Si_{III}—B\ , \tag{16}$$

where the subscript gives the coordination number and the superscript the charge state.

A ratio $C_B=8.5\times 10^{-6}$ is necessary to quench 10^{19} cm^{-3}neutral dangling bonds.[41] The reduction of neutral dangling bonds diminishes the interactions of the clusters with the $(SiH_2)_n$ interstitial chains, the viscosity is enhanced, and rotation of the clusters is favored.[8] This explains why V_g increases[7] by a factor of 4 in the range $(0-7)\times 10^{-6}$ of diborane and correspondingly why the density of neutral dangling bonds measured at room temperature decreases[7] from $10^{19}/cm^3$ to $10^{17}/cm^3$. When the crystallization occurs in the temperature range $550\,°C\leq T\leq 600\,°C$, the dangling-bond concentration is enhanced by a factor of 15 against its value at room temperature. This can be explained simply by the outdiffusion of hydrogen chemically bonded in the bulk. The dangling-bond concentration is however higher at the amorphous-crystalline interface: clusters of atoms in the amorphous phase have fewer dangling bonds per atom than nuclei of the same size,[34] and the dangling bonds in the vicinity of the interface are captured by it. If we envisage, following Brodsky and Döhler,[42] that the interfacial band structure is similar to that at a metal-semiconductor interface, in which the amorphous silicon behaves like a metal with a low density of states within the band gap, the Fermi level is pinned close to midband and the electrical conductivity σ is low,[40] about 10^{-7} $(\Omega\ cm)^{-1}$. To accommodate a Fermi level close to the valence band on the heavily doped crystalline side of the interface and a near midband Fermi level in the amorphous phase, there must be considerable band bending at the interface. The higher the doping level, and the higher the electric field at the interface, the better the capture cross section will be of dangling bonds (DB's) in the vicinity of the interface. According to Germain *et al.*,[13] the crystallization growth rate V_g can be expressed by the equation

$$V_g=\delta\nu_{DB}^{0}\exp(-E_{DB}/k_BT)\ , \tag{17}$$

where δ is the distance of the jump of a dangling bond from the *a* to the *c* side of the interface, ν_{DB}^{0} is a frequency characteristic of the capture of dangling bonds, ν_{DB}^{0} is an increasing function of charged-dangling-bond concentration, and E_{DB} is the activation energy for the diffusion of dangling bonds and/or the electrostatic barrier of their capture at the interface.

Consequently, we expect an enhancement of V_g with increasing the doping level up to $C_B=8.5\times 10^{-6}$. For $8.5\times 10^{-6}\leq C_B\leq 2.5\times 10^{-4}$, $C_B=2.5\times 10^{-4}$ is the solubility limit[43,41] of boron into silicon at 600 °C, the reaction (18) occurs during deposition according to Street:[12]

$$Si_{III}^{0}+B_{III}^{0}\rightleftharpoons B_{IV}^{-}+Si_{III}^{+}\ . \tag{18}$$

As the Fermi level moves in the gap, σ increases.[40] Because the band bending at the interface diminishes, consequently the electric field at the interface diminishes lowering the capture cross section of the dangling bonds at the interface; V_g is roughly constant.[7] This is consistent with Phillips' idea:[8] If all dangling bonds of submicrocrystallite edges are saturated with boron atoms, the viscosity can no longer diminish and V_g is constant.

For $2.5\times 10^{-6}\leq C_B\leq 2\times 10^{-3}$, alloying effects are expected, especially near the higher values of C_B. $E_v=4.1$ eV, V_g increases again,[7] and correspondingly σ increases up to about 10^{-1} $(\Omega\ cm)^{-1}$.

Dangling bonds are the most common defect in the bulk *a*-Si grown by CVD. The density of dangling bonds at the interface is very high ($\geq 10^{20}$ cm^{-3}). Is this dangling-bond concentration sufficient to create enough vacancies to enhance crystallization *via* mass transport controlled by the diffusion of the silicon self-interstitial[44,45] in the amorphous phase, as seems to be the case for crystallization of ion-implanted amorphous Si films?[46]

In this situation, crystallization occurs by moving kinks, as proposed by Williams and Elliman.[14] Our experimental V_g data[7] for boron-doped samples are therefore higher than those predicted by this latter model. The discrepancy can be explained by the fact that these authors do not take into account the charge state of a kink. A charged kink favors the crystallization by lowering their formation and migration energies.[47]

If the dangling-bond concentration at the interface is not sufficient, crystallization appears to be a consequence of bond breaking and bond rearrangement at the inter-

face. According to Germain *et al.*,[13] the capture cross section at the interface depends on the charge state of the dangling bonds and modifies the growth rate at this interface. The dangling bonds or floating bonds[48,49] move in the plane of the interface. Sites available for crystallization are those in the amorphous side of the interface which have captured a dangling bond. If available sites are kinks, the amorphous-crystalline interface can be regarded as a two-dimensional dislocation core.

V. CONCLUSION

From *in situ* x-ray diffraction measurements, we have been able to identify three different regimes during the solid-phase crystallization of *a*-Si CVD thin films deposited on fused-silica substrates. Transient surface-induced heterogeneous nucleation at the onset of the crystallization process has been experimentally demonstrated for the first time. It is followed by the growth of three-dimensional polycrystalline islands which merge at the substrate-film interface. The crystallization front then proceeds towards the surface of the film and the crystallized volume increases linearly with increasing annealing time. The role of the stresses at the *a*-Si-*c*-Si interface and the soft transverse acoustic phonon on solid-phase crystallization kinetics has been pointed out. The main result is therefore the indirect experimental evidence of strained submicrocrystallites in the amorphous phase prior to crystallization.

ACKNOWLEDGMENTS

The authors wish to thank Professor J. Bok for suggestions during discussion of the results. Thanks are due to Mr. C. Feuillebois for his technical assistance.

[1]K. Zellama, P. Germain, S. Squelard, J. C. Bourgoin, and P. A. Thomas, J. Appl. Phys. **50**, 6995 (1979).
[2]S. Squelard, K. Zellama, P. Germain, and B. Bourdon, Rev. Phys. Appl. **16**, 657 (1981).
[3]L. Csepregi, E. F. Kennedy, T. J. Gallagher, J. W. Mayer, and T. W. Sigmon, J. Appl. Phys. **48**, 4234 (1977).
[4]L. Csepregi, E. F. Kennedy, T. J. Gallagher, J. W. Mayer, and T. W. Sigmon, J. Appl. Phys. **49**, 3906 (1978).
[5]A. Lietoila, A. Wakita, T. W. Sigmon, and J. F. Gibbons, J. Appl. Phys. **53**, 4399 (1982).
[6]O. I. Reilly and W. E. Spear, Philos. Mag. **38**, 295 (1978).
[7]R. Bisaro, J. Magariño, K. Zellama, S. Squelard, P. Germain, and J. F. Morhange, Phys. Rev. B **31**, 3568 (1985).
[8]J. C. Phillips, J. Appl. Phys. **59** (2), 383 (1986).
[9]J. C. Phillips, J. C. Bean, B. A. Wilson, and A. Ourmazd, Nature **325**, 121 (1987).
[10]A. Ourmazd, J. C. Bean, and J. C. Phillips, Phys. Rev. Lett. **55**, 1599 (1985).
[11]R. Bisaro, J. Magariño, N. Proust, and K. Zellama, J. Appl. Phys. **59**, 1167 (1986).
[12]R. A. Street, Phys. Rev. Lett. **49**, 1187 (1982).
[13]P. J. Germain, M. A. Paesler, and K. Zellama, in *Cohesive Properties of Semiconductors Under Laser Irradiation,* Vol. E69 of *NATO Advanced Study Institute, Series E: Applied Sciences,* edited by L. D. Laude (Nijhoff, The Hague, 1983), p. 506.
[14]J. S. Williams and R. G. Elliman, Phys. Rev. Lett. **51**, 1069 (1983).
[15]J. S. Johannessen, Phys. Status Solidi A **26**, 571 (1974).
[16]W. E. Spear, G. Willeke, P. G. Le Comber, and A. G. Fitzgerald, J. Phys. (Paris) Colloq. **42**, C4-257 (1981).
[17]J. F. Morhange, thèse de troisième cycle, Université de Paris VI, 1972.
[18]S. Veprek, Z. Iqbal, and F. A. Sarott, Philos. Mag. B **45**, 137 (1982).
[19]R. Bisaro, N. Proust, J. Magariño, and K. Zellama, Thin Solid Films **124**, 171 (1985).
[20]Y. Pastol, R. Bisaro, N. Proust, J. Magariño, J. Von Bardeleben, K. Zellama, P. Germain, and S. Squelard (unpublished).
[21]D. Turnbull, in *Solid State Physics, Advances in Research and Applications,* edited by F. Seitz and D. Turnbull (Academic, New York, 1956), Vol. 3, p. 225.
[22]D. Turnbull, J. Chem. Phys. **18**, 198 (1950).
[23]P. Germain and K. Zellama, in Ref. 13, p. 254.
[24]K. Zellama, P. Germain, P. A. Thomas, and A. Gheorghiu, in Ref. 13, p. 279.
[25]J. W. Christian, in *Physical Metallurgy,* edited by R. W. Cahn (North-Holland, Amsterdam, 1970), Chap. 10.
[26]M. Avrami, J. Chem. Phys. **7**, 1103 (1939).
[27]M. Avrami, J. Chem. Phys. **8**, 212 (1940).
[28]S. Veprek, Z. Iqbal, H. R. Oswald, F. A. Sarrott, J. J. Wagner, and A. P. Webb, Solid State Commun. **39**, 509 (1981).
[29]F. Spaepen, Philos. Mag. **30**, 417 (1974).
[30]M. L. Rudee and A. Howie, Philos. Mag. **25**, 1001 (1972).
[31]R. W. Kilb and L. Pierce, J. Chem. Phys. **27**, 108 (1957).
[32]G. H. Döhler, R. Dandoloff, and H. Bilz, J. Non-Cryst. Solids **42**, 87 (1980).
[33]W. Weber, Phys. Rev. B **15**, 4789 (1977).
[34]R. Mosseri and J. F. Sadoc, J. Non-Cryst. Solids **77** and **78**, 179 (1985).
[35]J. T. Randall, H. P. Rooksby, and B. S. Cooper, Nature **125**, 458 (1930).
[36]K. S. Evstropyev and E. A. Porai-Koshits, J. Non-Cryst. Solids **11**, 170 (1972).
[37]W. H. Zachariasen, J. Am. Chem. Soc. **54**, 3841 (1932).
[38]J. C. Phillips, Phys. Rev. Lett. **42**, 1151 (1979).
[39]J. C. Phillips, J. Non-Cryst. Solids **34**, 153 (1979).
[40]R. Bisaro, E. Chartier, D. Kaplan, J. Magariño, N. Proust, and N. Szydlo, Rev. Tech. Thomson-CSF **15**, 321 (1983).
[41]J. Magariño, D. Kaplan, A. Friederich, and A. Deneuville, Philos. Mag. B **45**, 285 (1982).
[42]M. H. Brodsky and G. Döhler, CRC Crit. Rev. Solid State Mater. Sci. **5**, 592 (1975).
[43]F. A. Trumbore, Bell Syst. Technol. J **39**, 205 (1960).
[44]J. Narayan, J. Appl. Phys. **53**, 8607 (1982).
[45]J. C. Bourgoin and R. Asomoza, J. Cryst. Growth **69**, 489 (1984).
[46]Y. Pastol, R. Bisaro, N. Proust, and J. Magariño, Rev. Tech. Thomson-CSF **19**, 373 (1987).
[47]R. Jones, Philos. Mag. B **42**, 213 (1980).
[48]S. T. Pantelides, Phys. Rev. Lett. **57**, 2979 (1986).
[49]S. T. Pantelides, Phys. Rev. Lett. **58**, 1344 (1987).